Baseline Design of a 16 T $\cos\theta$ Bending Dipole for the Future Circular Collider

R. Valente, G. Bellomo, B. Caiffi, P. Fabbricatore, S. Farinon, S. Mariotto, A. Pampaloni, A. M. Ricci, M. Sorbi, M. Statera

***Abstract*—The EuroCirCol project is part of the FCC study under the European Union leadership in the framework of a H2020 project. In particular the Italian Institute for Nuclear Physics (INFN), in collaboration with CERN and other European laboratories, is developing the design of a cos-theta Nb_3Sn dipole magnet which will be part of the Conceptual Design Report (CDR) of the FCC studies in 2019. The magnet, with an aperture diameter of 50 mm and a bore field of 16 T, will be able to bend the beams at final energies and within collider size constraints. Here we present an update of the electromagnetic design of the Nb_3Sn cos-theta dipole in double-aperture configuration, the 2D mechanical analysis and also the 3D coil ends study.**

***Index Terms*—Accelerator dipoles, superconducting magnets, Nb_3Sn, magnetic design.**

I. Introduction

EuroCirCol [1] is the project co-financed by the European Union which aims to develop a conceptual design study of the Future Circular Collider (FCC) [2], that is a 100 km circumference collider of 50 TeV proton beams, that represents the future of High Energy Physics machines in the post-LHC era.

The INFN groups in Milan (L.A.S.A.) and Genoa are responsible for studying a 16 T cos-theta bending dipole design, which will be the baseline option of CDR to be issued in 2019. This twin-aperture dipole can reach 16 T field using four Nb_3Sn conductor layers. For the FCC target, Nb_3Sn superconducting properties are needed, but due to its brittleness it is a frontier technology for accelerator magnets. Therefore, the development and construction of very high field magnets are the most challenging aspects of FCC design also for cost reasons [3].

In this paper we describe the main updates of the cross-section layout in terms of iron shape and coil configuration. In particular, we deduce a new yoke with an insert between apertures which is able to reduce the b_2 wide variation of the previous design [4]. Moreover, we explain why the cold mass size constraint implies an asymmetric cos-theta coil configuration, in order to compensate the strong interaction between apertures. We also present both electromagnetic and mechanical analysis, showing that field quality is within the requirements and the technical feasibility of the Bladder & Keys technology for this magnet. Finally, studies on 3D coil ends design is mentioned for the new asymmetric coil configuration.

This work was supported by the European Union's Horizon 2020 research and innovation programme under grant No 654305, EuroCirCol project.

G. Bellomo and S. Mariotto, M. Sorbi are with the University of Milan, Milan 20122, Italy and also with INFN-L.A.S.A, Milan 20090, Italy

R. Valente and M. Statera are with INFN-L.A.S.A, Milan 20090, Italy (email: riccardo.valente@mi.infn.it).

B. Caiffi, P. Fabbricatore, S. Farinon and A. Pampaloni are with INFN-Genova, Genova 16146, Italy

A. M. Ricci is with University of Genoa, Genoa 16146, Italy and also with INFN-Genoa, Genoa 16146, Italy.

II. Magnet design

The magnetic design and harmonic analysis have been performed using ROXIE 10.2 [5].

A. Design parameters

After studies on different bending dipole designs [6], [7], a final decision was taken to make the design compatible for installation in the existing LHC tunnel, in order to use the same magnet design for both FCC and High Energy LHC (HE-LHC). Since the maximum outer cryostat diameter allowed is then 1215 mm, the cold mass diameter must be set accordingly. For this reason, in the previous version of the conceptual design [4], [8], the yoke diameter has been reduced from 800 mm to 600 mm and the inter-beam distance has been decreased from 250 to 204 mm. Further studies have shown that yoke size and inter-beam distance have a great influence in field quality, because the cross-talk between the two apertures induces systematic multipoles extremely difficult to correct, especially b_2 and b_3. In particular, it resulted that b_2 component was not acceptable for an accelerator magnet field quality (b_2 variation > 40 units), therefore some design parameters were modified to meet the requirements, which are summarized in Table I [6], [7]: the inter-beam distance and the iron yoke diameter have been increased respectively to 250 mm and 660 mm, in order to reduce as much as possible the cross-talk effect [9]. Furthermore, for mechanical purpose the iron yoke is enclosed in an Al alloy shell 50 mm thick to provide the additional and final pre-stress in coils during cool down and everything is bound together by a steel shell 20 mm thick which works as vessel. The whole cold mass diameter is 800 mm, taking into account that the cryo-system size will be optimized to satisfy the LHC tunnel compatibility (see Fig. 6 for further details).

B. Cross-section layout and field quality

In this section we describe step by step how we obtained the new baseline design of the 16 T dipole, on the basis of the changes in the design parameters. The cross-section

TABLE I
MAIN DESIGN REQUIREMENTS

Bore inner diameter	50 mm
Beam distance	250 mm
Material	Nb_3Sn
Bore nominal field	16 T
Operating temperature	1.9 K
J_c (@ 1.9 K, 16 T)	2415 A mm^{-2}
Operation on the load-line	86%
Maximum number of strands	40
Insulation thickness	0.15 mm
Cu/Non-Cu	≥ 0.8
Field harmonics (geometric/saturation)	$\leq 3/10$ units
Iron yoke outer radius	330 mm
Number of apertures	2
Length	14.3 m

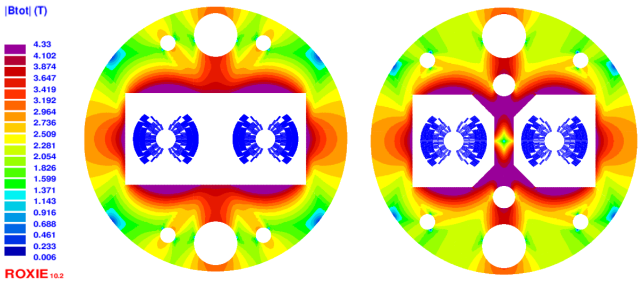

(a) Previous design. (b) New design.

Fig. 1. Comparison between iron yoke before and after optimization. The modulus of the magnetic field is plotted at operating current.

shown in Fig. 1a is the starting point iron shape obtained increasing the yoke diameter and the inter-beam distance of the previous configuration [4] as described in section II-A. The two apertures are assembled inside a rectangular window of the iron yoke; each of them is made of four double pancakes connected in series. The field quality of this layout is not yet satisfactory, because of b_2 and b_3 wide values at injection and collision energy, as you can see in Fig. 2. In order to optimize

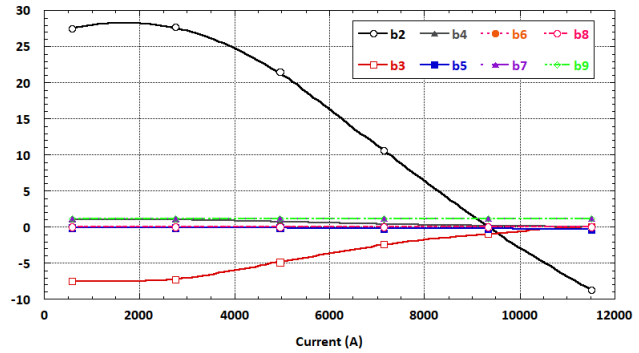

Fig. 2. Field quality of the magnet with the previous design iron yoke (Fig. 1a) and the symmetric coil configuration presented in [4].

the iron shape according to the field quality requirements, we obtain the iron yoke shown in Fig. 1b. The iron insert between apertures works as a pole and is able to decrease the b_2 variation from 35 units to 6 units. Nevertheless, there is an offset of about -35 units which could not be eliminated with iron shaping only, taking into account that it is mandatory using flat interfaces wide enough to adopt the Bladder & Keys technology between the iron yoke and the steel pad. Therefore,

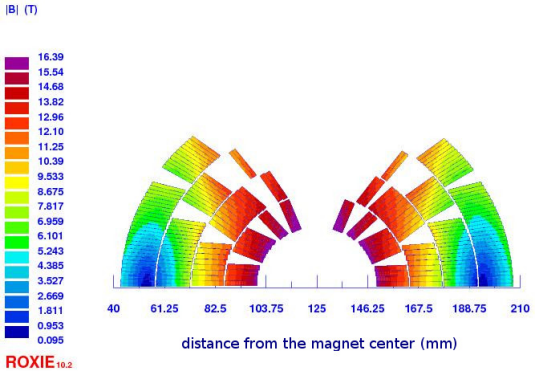

Fig. 3. New asymmetric coil arrangement after Roxie optimization.

we decided to compensate the cross-talk effect, breaking the left-right symmetry in each cos-theta aperture, modifying the geometric coil configuration and maintaining the same iron yoke shown in Fig. 1b. The asymmetric coil configuration has been achieved using the Extreme algorithm of the Roxie optimizer, changing phi and alpha angles as design variables (phi defines the angular position of the first conductor of each block, alpha is its tilting angle with respect to the horizontal). The post-optimization coil windings are shown in Fig. 3, and the main cable parameters are reported in Table II. The two

TABLE II
CONDUCTOR FEATURES

	HF conductor	LF conductor
Strand diameter (mm)	1.1	0.7
Number of strands	22	38
Material	Nb_3Sn	Nb_3Sn
Bare width (mm)	13.2	14
Bare inner thickness (mm)	1.892	1.204
Bare outer thickness (mm)	2.0072	1.3261
Insulation thickness (mm)	0.15	0.15
Keystone angle	0.5°	0.5°
Cu/Non-Cu	0.82	2.08
Operating current (A)	11441	11441
Operating point on Load Line (1.9 K)	86.0%	85.8%
Peak field (T)	16.4	12.71

inner layers are made of High Field conductor (HF) whereas the two outer layers of Lower Field conductor (LF), because the "grading" technique is used to maximize the main field in the bore. The minimum tip thickness of the wedge in contact with the mandrel is 0.74 mm, located between first and second block of the first layer on the right side of the aperture. The conductor parameters are the same as the previous conceptual design [4], but the operating current has been increased to 11441 A to restore the bore field to 16 T. The operating point on the load-line has more than 14% margin both for LF and HF

cables, which is the minimum conventional value determined by EuroCirCol collaboration (see Table II).

Regarding the field quality, the asymmetric coil allows to remove the b_2 offset mentioned above; moreover both b_2 and b_3 components fulfill any requirement. In fact, at injection they are far below the threshold of 10 units, and at collision energy each harmonic is not far from zero (see Fig. 4 and Table III).

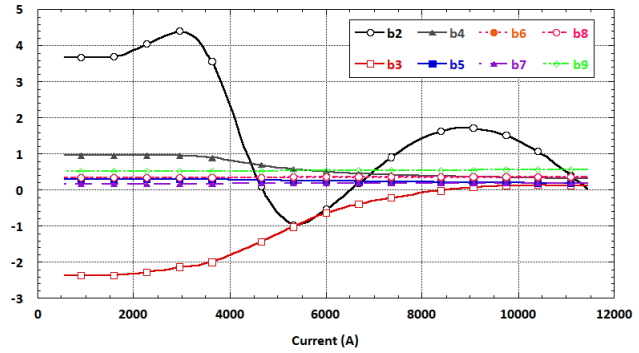

Fig. 4. Field quality of the magnet with the new iron yoke (Fig. 1b) and the optimized asymmetric coil arrangement (Fig. 3).

TABLE III
HIGH ORDER HARMONICS AT OPERATING CURRENT

b_2	b_3	b_4	b_5	b_6	b_7	b_8	b_9
0.025	0.106	0.31	0.18	0.35	0.18	0.37	0.57

C. Quench Protection

The magnet quench protection is a challenging aspect due to the large stored energy volumetric density and therefore accurate studies have been performed for the previous magnet configuration [10], [11]. The collaboration agreed to define 20 ms to detect the quench and 20 ms to quench protection being effective, with the requirement to keep the hotspot temperature ($T_{hotspot}$) below 350 K and the maximum voltage toward ground (V_{gnd}) below 1.2 kV, when the current is 105% of the operating current. These values are determined by the Hi-Lumi experience with Nb_3Sn [12]. Last quench protection analysis are performed considering Quench Heaters (QH) or alternatively Coupling-Loss Induced Quench system (CLIQ), and both of them allow to satisfy the above requirements [13]. The results are summarized in Table IV.

TABLE IV
QUENCH SIMULATION RESULTS.

Device options	$T_{hotspot}$(K)	V_{gnd} (V)
QH	322	870
CLIQ	286	800

III. COIL ENDS DESIGN

A first design of the coil ends was studied in [4], for both the side opposite to connections and the connection side, using the ROXIE code. The reported update of the cross section required a new design. The optimized 3D model of the side opposite to connections is shown in Fig. 5. The main requirements of the optimization were the length of each coil end to be kept within 300 mm and the peak field in the end to be kept 0.2 T lower than the one in the corresponding straight part. To

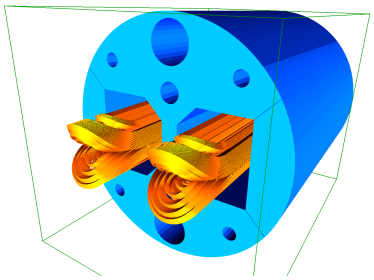

Fig. 5. Double aperture $\cos\theta$ design of the side opposite to connections in ROXIE. Coils are represented in yellow, iron yoke in blue.

ease the computation, we did a model with a magnetic length arbitrarily shorter than the design one. The straight section and the iron yoke are 1.58 m and 1.5 m long respectively. The coil extremity begins 40 mm after the end of the yoke. This is a good solution to reduce the peak field in the end without spacing out too much the blocks. The minimal longitudinal distance between the blocks is about 5 mm and the maximum about 31 mm. To ensure that there are no uncompressed straight parts, all layers begin to bend nearly in the same longitudinal position. Each coil end is 152 mm long and the overall length of the model is 1.884 m. The resulting magnetic length is 1.74 m. The field quality obtained is shown in the first row of Table V. The second line displays the integrated harmonics predicted for a magnet with a magnetic length of 14.3 m. The values are derived by the formula

$$\bar{b}_n = \frac{\bar{b}_{n,\,short}\, L_{m,\,short} + b_n(z=0)\,(L_m - L_{m,\,short})}{L_m} \quad (1)$$

where $\bar{b}_{n,\,short}$ are the integrated harmonics in the short model (see Table V), $L_{m,\,short} = 1.74$ m is the magnetic length of the short model and $L_m = 14.3$ m is the magnetic length of the final magnet. The peak fields in the high and low field

TABLE V
INTEGRATED HARMONICS AT OPERATING CURRENT.

L_m	$\bar{b}_2$	$\bar{b}_3$	$\bar{b}_4$	$\bar{b}_5$	$\bar{b}_6$	$\bar{b}_7$	$\bar{b}_8$
1.74 m	-7.3	-6.92	0.4	0.08	0.37	0.21	0.38
14.3 m	-0.87	-0.75	0.32	0.17	0.35	0.18	0.37

regions are computed by ROXIE and the values obtained are reported in Table VI. It is worth noting that, as it was required by the project, the peak fields in the straight part are at least 0.2 T larger than in the coil end.

TABLE VI
PEAK FIELDS IN 3D MODEL AT OPERATING CURRENT.

Conductor	Cross section	Coil end
LF	12.7 T	12.5 T
HF	16.4 T	15.4 T

IV. MECHANICAL DESIGN

In this section, the mechanical design of the CDR baseline is presented. The characteristics of the new design are described in detail, focusing on the main differences with respect to the previous baseline, reported in [4]. The results of the FE analysis are also reported, showing that they fulfill all the project requirements. Previous studies of the mechanics are reported in [14].

A. Mechanical design parameters

The optimization of the field quality required a certain number of modifications, the main one being the increase of the inter-beam distance from 204 mm to 250 mm, in order to reduce the magnetic cross talk between the two apertures. This main modification, beside the requirement of keeping the compatibility with the LHC tunnel, lead to several changes in the design, as it can be seen from the comparison in Fig. 6. Dimensions of the new CDR baseline are shown in Fig.7. The main modifications are listed below:

- an iron wall with a particular pole shape was added between the two apertures, to optimize further the field quality;
- the outer diameter of the iron yoke was enlarged from 600 mm to 660 mm, to accomodate the new inter-beam distance;
- the thickness of the aluminum ring was reduced from 70 to 50 mm to make the magnet more compact and keep the compatibility with the LHC tunnel. To guarantee the required level of pre-stress in this configuration, the outer steel shell was assumed to be soldered in compression;
- A loading plate (i.e. a flat stainless steel sheet aligning all the four layers) was introduced to give pre-compression to the coil in a more uniform and efficient way, and the shape of the titanium pole was modified accordingly.

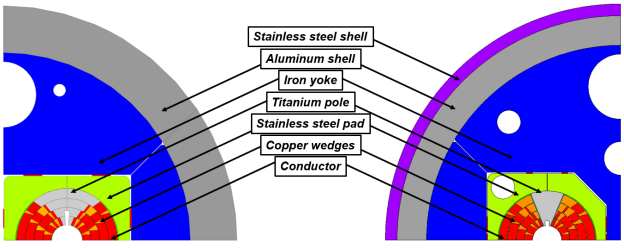

Fig. 6. Comparison between the previous baseline (on the left) and the CDR baseline (on the right).

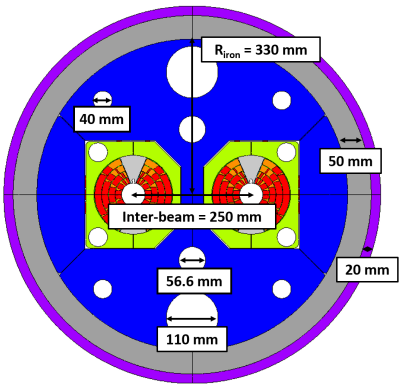

Fig. 7. Main dimensions of the CDR baseline design.

B. Mechanical constraints

The mechanical requirements agreed from the EuroCirCol [1] collaboration are listed below:

- the VM stress in the conductors must be lower than 150 MPa at room temperature and 200 MPa at cryogenic temperatures;
- the VM stress in the mechanical structure must not exceed the values reported in Table VII, which already take into account safety factors with respect to the yield strength of the material;
- the pole-coil contact pressure in pole-turns midpoint should be larger than 2 MPa and the average contact pressure per each layer should be larger than 0.

TABLE VII
STRESS LIMIT ON THE MATERIALS OF THE STRUCTURAL COMPONENTS.

Material	Stress limit @RT [MPa]	Stress limit @1.9 K[MPa]
Ti6Al4V	800	1650
Austenitic Steel	350	1050
Ferromagnetic Iron	230	720
Al7075	480	690

The last requirement was set to avoid unwanted movements between the coil and the pole, which could cause local heat because of the friction and trigger a quench. These movements can occur in particular during the energization, because of the Lorentz forces which tend to push the coils outward in the radial direction and toward the midplane in the azimuthal direction. A suitable pre-compression must be given to the coils in order to take them in position during the current charge.

In this project, it is assumed that the pre-stress will be given using the “Bladder & Key” concept, a rather new technique introduced in [15]. With this technique, the assembly of the magnet is performed as follows: coils, stainless steel pad and aluminum shell are assembled using keys with some interference, in order to give already at room temperature pre-compression to the coils. Additionally, the outer stainless steel shell is soldered under compression, so to compensate the

mentioned Al shell thickness reduction of the baseline design. When the system is cooled down, the aluminum shell shrinks more than the inner components, giving additional pre-stress. In this way, most of the pre-compression is given at cryogenic temperatures, where Nb_3Sn exhibits better mechanical properties. Fig. 8 shows an enlargement of the keys region, with indication of bladder positions. Due to the irregular pad/yoke shape, the inner vertical key has no interference; the total interference has been attributed to the right vertical key and corresponds to 1.2 mm. The bladder pressure needed to open those interference gaps is 60 MPa. The horizontal keys are much less critical, having an interference of only 0.2 mm.

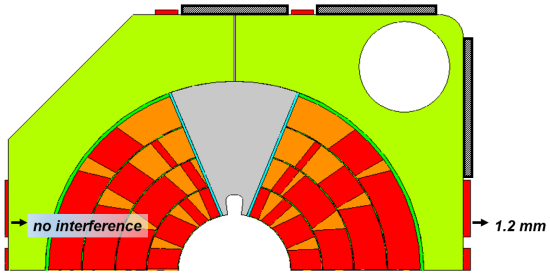

Fig. 8. Enlargement of the keys region, with indication of bladder positions.

C. FEA results

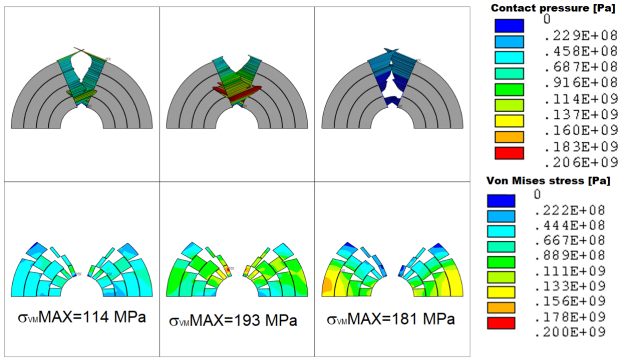

Fig. 9. Contact pressure between the coil and the pole (upper row) and Von Mises stress in the conductor (lower row) after assembly (left), cool down (center) and energization to 16 T (right).

A mechanical model was prepared with FE code ANSYS [16] including all the relevant geometrical details. The material properties for the structural components can be found in [14]. The four layers are assumed to be glued together, including the wedges. This possibly implies that the four layers are impregnated together, but to definitely set how to construct and assemble the two double pancakes an intense R&D activity has been funded and is foreseen in the next years. The coil and the titanium pole can slide (with a friction coefficient of 0.2) and detach from each other. The same kind of contact surfaces were also defined between the keys, the iron yoke, the aluminum ring and the steel shell. The simulation reproduces the following three main steps: the assembly of the magnet,

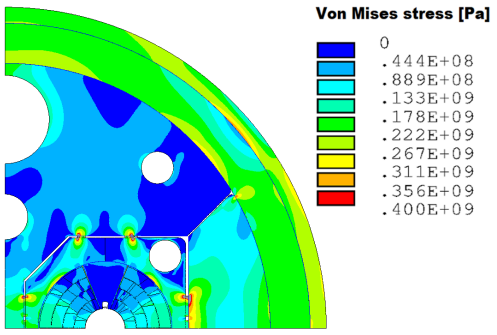

Fig. 10. Von Mises stress in the structural components after energization to 16 T.

which includes the insertion of the keys and the closing of the steel shell in pressure, the cool down and the energization to 16 T. The results regarding the VM stress in the conductor and the contact pressure between the coil and the pole are shown in Fig. 9: the stress is below the acceptable limit in all the calculation steps. The requirements on the pole-coil contact pressure are also satisfied. As the coil are not glued to the pole, a small gap of 2 μm opens in that region, but it can be considered negligible. The asymmetry in the coil position does not introduce any issue from the mechanical point of view. The radial displacement of the midplane turns goes from -85.6 μm to 226 μm from energization to cool-down and this will be taken into account during the coil construction to not affect the field quality. The stress on the mechanical structures are shown in Fig. 10. For sake of simplicity, the results are shown only after energization. The level of stress was found to be lower than the limits, except for very localized hot spots under the keys, where interference cause plasticization to occur, but without compromising the effectiveness of the structure.

V. Conclusions

We have presented the latest design of the 16 T cos-theta bending dipole for FCC, which will be the baseline configuration for the CDR in 2019.

The magnet has been developed by the INFN team of EuroCirCol, and it is able to stay within any constraint approved by the collaboration. In fact, the bore field of 16 T is reached without exceeding the margin limit of 86% on the Load Line, both for HF and LF cables. Moreover, 2D and 3D harmonic analysis show that field quality fulfills any requirements, in particular each multipolar component is below 4.5 units at injection and not far from zero at collision energy.

The mechanical analysis indicates that the Bladder & Keys solution is effective in maintaining stresses on conductors and mechanical structure below the Nb_3Sn degradation threshold, i.e 150 MPa at room temperature and 200 MPa at 1.9 K, apart from very localized hotspots under the keys. Finally, the new common loading plate for all four layers ensures a positive contact pressure between pole and coils, for each magnet work phases.

REFERENCES

[1] http://www.eurocircol.eu/

[2] https://home.cern/about/accelerators/future-circular-collider

[3] D. Schoerling et al., Consideration on the Cost Model for High-Field Dipole Arc Magnets for FCC, IEEE Trans. on Applied Superc., Vol. 27, no. 4, 2017, art. no. 4003105

[4] V. Marinozzi, G. Bellomo, B. Caiffi, P. Fabbricatore, S. Farinon, A. Ricci, M. Sorbi, M. Statera, "Conceptual Design of a 16 T cos θ Bending Dipole for the Future Circular Collider", Applied Superconductivity IEEE Transactions on, vol. 28, no. 3, pp. 1-5, 2018.

[5] S. Russenschuck, Field Computation for Accelerator Magnets: Analytical and Numerical Methods for Electromagnetic Design and Optimization. Weinheim, Germany: Wiley, 2010.

[6] D. Tommasini et al., The 16 T dipole development program for FCC, IEEE Trans. Appl. Supercond., vol. 27, no. 4, Jun. 2017, Art. no. 4000405.

[7] D. Tommasini et al., Status of the 16 T dipole development program for a future hadron collider, IEEE Trans. Appl. Supercond., vol. 28, no. 3, Apr. 2018, Art. no. 4001305.

[8] M. Sorbi et al., The Eurocircol cosine-theta Dipole Option for FCC, IEEE Trans. on Applied Superc., Vol. 27, no. 4, 2017, art. no. 4001205

[9] D. Schoerling et al., The 16 T Dipole Development Program for FCC and HE-LHC, presented at this Conference 1LOr1D-03, to be published at IEEE Trans. on Applied Superc., 2019

[10] V. Marinozzi et al., "Quench Protection Study of the Eurocircol 16 T Cosθ Dipole for the Future Circular Collider (FCC), IEEE Trans. on Applied Superc., Vol. 27, no. 4, 2017, art. no. 4702505

[11] J. Zhao et al., Mechanical stress analysis during a quench in CLIQ protected 16 T dipole magnets designed for the future circular collider, Physica C: Superconductivity and its Applications Volume 550, 15 July 2018, Pages 27-34, https://doi.org/10.1016/j.physc.2018.04.003

[12] E. Todesco, "Quench limits in the next generation of magnets" CERN Yellow Report 2013-006 10-16 (2013).

[13] T. Salmi et al., Quench Protection of the 16 T Nb3Sn Dipole Magnets Designed for the Future Circular Collider, presented at this Conference 3LPo2E-03 [L42], to be published at IEEE Trans. on Applied Superc., 2019

[14] B. Caiffi, G. Bellomo, P. Fabbricatore, S. Farinon, V. Marinozzi, A. Ricci, M. Sorbi, "Update on Mechanical Design of a Cosθ 16-T Bending Dipole for the Future Circular Collider", Applied Superconductivity IEEE Transactions on, vol. 28, no. 4, pp. 1-4, 2018.

[15] S. Caspi, S. Gouraly, R. Hafalia, A. Lietzke, J. ONeill, C. Taylor, A. Jackson, "The use of pressurized bladders for stress contol of superconducting magnets", Applied Superconductivity IEEE Transactions on, vol. 11,6948843, 2002.

[16] https://www.ansys.com/